PREDICTION OF CONDUCTED RFI EMISSIONS IN BLDC MOTORS FOR AUTOMOTIVE APLICATIONS

J. E. Makaran
Siemens Automotive Inc.
1020 Adelaide St. S.
London, Ontario, N6E 1R6, CANADA

J. LoVetri
Department of Electrical and Computer Engineering
University of Manitoba
Winnipeg, Manitoba, R3T5V6, CANADA

Abstract: With the proliferation of electronic devices in automobiles, an emphasis has been placed on EMC issues for among others reasons, safety. The EMC design cycle can be lengthy, with the mitigation of conducted RFI emissions still largely a trial and error process. The use of a virtual motor and drive model can be used to shorten this process. In the modeling of conducted RFI emissions, an accurate model of motor and drive is necessary. Furthermore, a representative method of characterizing the conducted RFI spectrum is required. A virtual motor model for an electronically commutated engine cooling fan motor and drive is presented to predict conducted RFI emissions up to 30 MHz. This model forms the basis of a method that may be used to predict conducted RFI emissions on other motor and drive types.

Introduction

With an increase in the capability of electronic modeling tools, simulation models of motors and drive systems can be supplied to an automaker prior to actual sample parts. A virtual electromechnical system comprised of "parts" can be used to predict system behavior to identify problems associated with alternator and battery loading, as well as wiring harness and fuse sizing prior to system builds. Although not presently required, virtual modeling of motors can extend to the prediction of conducted RFI emissions.

Motors are analogous to transformers in that, high frequency motor models must include accurate models of elements such as self and mutual coupling between the motor phases, iron losses, as well as accurate models of the associated drive and load.

Several published papers have dealt with the prediction of conducted RFI emissions associated with brush type [1-2] and brushless motors [3-8] for automotive and industrial applications. Publications pertaining to brushless applications typically examine the relationship between motor and drive for high voltage, three phase bipolar motors for use in electric vehicle or industrial applications. As such, there are no papers examining conducted RFI emissions from low voltage, high current, unipolar permanent magnet motors. This paper considers the simulation of conducted RFI emissions from a 13 V, 400W, five phase, permanent magnet, unipolar, brushless DC motor for use in an underhood automotive engine cooling application.
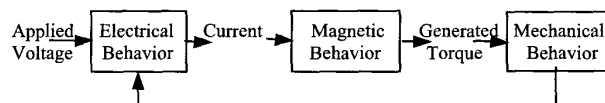
Model Formulation

The system which was modeled is depicted in Figure 1.
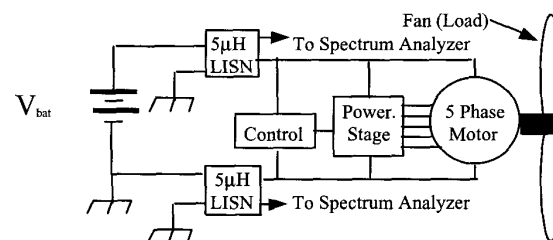
Figure 1. Schematic representation of system model.

In the formulation of the system model, the relationship between the electrical and mechanical behavior of the motor and load was considered. This relationship is represented in block form in Figure 2.

Figure 2. Relationship between electrical, magnetic, and mechanical system behavior.

The electrical behavior of the machine is described by:

$$v = r^{T} i + d/dt \, L(\theta_r) \, i \qquad (1)$$

The applied voltage vector, v represents the voltage applied to the terminals of the motor (V). In the case where pulse width modulation (PWM) is used to control the speed of the motor, v will be a function of the PWM duty cycle. At full speed, the motor terminals will see the full battery voltage (PWM duty cycle = 100%).

The vector r represents the DC resistance vector of the motor phases (Ω). The rotor position is represented by θ_r (rad). $L(\theta_r)$ is the motor inductance matrix as a function of rotor position (H). The inductance matrix will include self and

mutual inductance terms. The phase current vector is represented by *i* (A).

The magnetic behavior of the machine is governed by:

$$T_e = P/2 \,[1/2 \, i^T \, d/dt \, L(\theta_r) \, i + \, i^T \, d/dt \, \lambda_m \,(\theta_r)] \qquad (2)$$

where the generated electromagnetic torque is represented by T_e (Nm)., P is the number of poles present in the machine (dim.), and $\lambda_m (\theta_r)$ is the flux with respect to rotor position (Wb).

The mechanical behavior of the machine is governed by:

$$T_e = J \,(2/P) \, d^2\theta_r \,/dt^2 + B_m \,(P/2) \, d\theta_r/dt + T_L \qquad (3)$$

Where J is the moment of inertia of the motor rotor and fan load (kg/m/s^2), B_m represents the iron and damping losses of the motor (kg m s/rad), and T_L represents the motor load (Nm).

For the case of a fan load:

$$T_L = (\omega_m)^2/K_{fan}^{\,2} \qquad (4)$$

The motor shaft speed is represented by ω_m (rad s^{-1}),while K_{fan} is the fan load constant (rad s^{-1}/ Nm $^{0.5}$).

By solving equations (1) – (3), the transient and steady state behavior of the machine can be determined. In the prediction of conducted RFI emissions, the steady state behavior under load conditions is the behavior of concern. An analytical approach to solving the equations has been used in the past to model low-frequency behavior of motors and their associated loads. The equations governing the behavior of a three phase machine have been solved using the Runge-Kutta technique [9-12]. In a similar manner, real time simulation of induction motors have been performed. Authors such as Strahan [13], Zhang et al: [14], Jack et al: [15-16] and Cho [17], to name a few, have created similar motor models for the study of motor performance, and low frequency issues of interest such as the prediction of torque ripple and acoustic noise.

Many authors have created models to study the performance of electronically commutated motors; the same cannot be said of the modeling of motors and drives in an attempt to predict conducted RFI emissions. Most of the work in this area has been performed only over the last six years.

Although publications dealing with brushless applications examine the relationship between motor and drive for high voltage, three phase bipolar induction motors for use in electric vehicle or industrial applications, there are no papers examining conducted RFI emissions from low voltage, high current, permanent magnet motors. In low voltage, high current applications, magnetic non-linearities and device parasitics cannot be ignored.

In order to attempt to model the high frequency behavior of the machine, drive, and associated load, an analytical

solution is not possible. Although an analytical approach can be effective in predicting the low frequency behavior of the machine, to predict the high frequency behavior of the system, bulk and parasitic elements of active and passive components in the inverter must be included. This would make an analytical solution extremely difficult. For simplicity, and to include parasitic terms present in electronic components such as diodes and MOSFET's, the entire system was modeled in PSPICE®. The magnetic behavior of the machine and the fan load were determined empirically and incorporated in the model. As such, the model employed was a lumped parameter model where the parameters were measured. Although all of the magnetic parameters such as the back EMF constants, self and mutual inductances were measured, they could have been predicted using numerical techniques such as a finite element method. Once the magnetic parameters were obtained, the magnetic behavior of the motor was adapted for the fan load across the entire operational speed range of the system. The system was modeled omitting significant RFI suppression components to decrease the sensitivity of the model to the characteristics of these components.

As conducted emissions testing to the specification of concern (a CISPR25 variant) was specified at a constant mid speed and constant high speed, the conducted emissions in the model were simulated at these speeds and compared with experimentally obtained results. In the present application, this corresponds to speeds of 1800 rpm, and 2600 rpm, respectively.

Time Domain Results

Time domain results provide a valuable qualitative validation of the system model. In comparing simulated and experimental results, the voltages of concern were the ones at the output of the Line Impedance Stabilization Network (LISN). The simulated negative LISN voltage at mid speed is shown in Figure 3. The actual measured negative LISN voltage for mid speed conditions is shown in Figure 4.
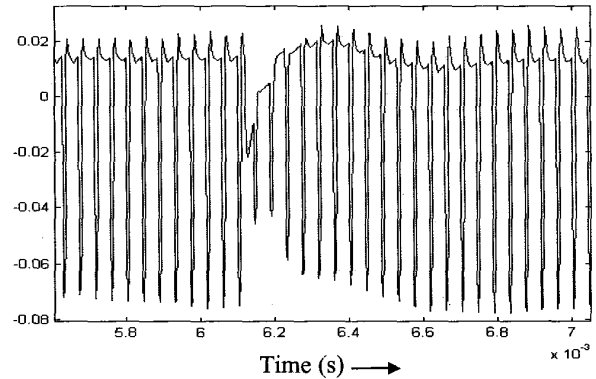

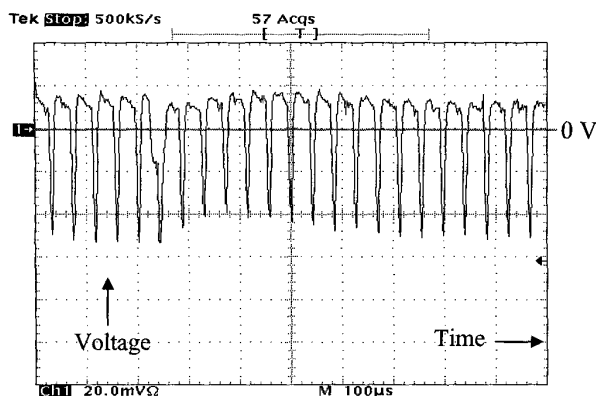Figure 3. Simulated negative LISN voltage at mid-speed.

22

Figure 4. Actual negative LISN voltage at mid-speed.

As may be seen in the waveforms for the mid speed case, the correlation between simulated and experimental waveforms is good, both in terms of magnitude as well as shape.

The same good correlation was seen for the high-speed case. The simulated negative LISN voltage at mid speed is shown in Figure 5. The actual negative LISN voltage for high speed conditions is shown in Figure 6.
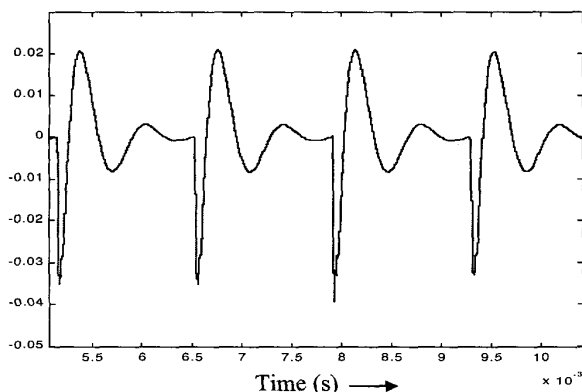

Figure 5. Simulated LISN voltage at high speed.
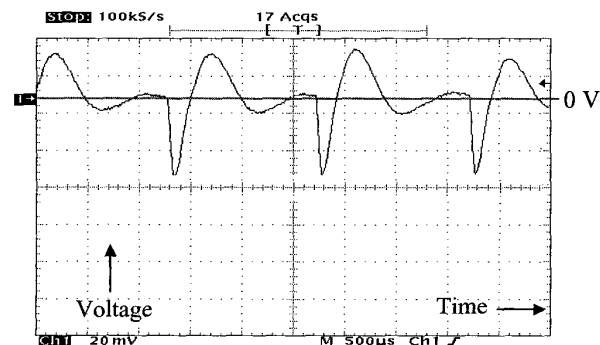

Figure 6. Actual LISN voltage at high speed.

It was also observed that the low frequency behavior of parameters such as phase currents, and drain to source voltages of MOSFET's, there was also a strong correlation between the simulated and actual results.

Once the time domain LISN voltages were obtained, a method of determining the frequency spectrum of the LISN voltages had to be implemented.

Determination of Conducted RFI Spectrum

The next step was to determine the conducted RFI spectrum of the LISN voltages. A virtual spectrum analyzer had to be simulated in a similar manner as the spectrum analyzer used to perform the experiments.

It is known that traditional spectrum analyzers operate on the heterodyne principle. To duplicate a heterodyne type spectrum analyzer in PSPICE® would be impractical due to long computing times. An alternate method attempted, was the implementation of a digital bandpass filter, whose characteristics approximated those of the IF filter of the spectrum analyzer used in obtaining the experimental results. The center of the filter was swept across the frequency band of interest in discrete frequency steps. The digital filter was applied to the LISN voltage waveforms for each frequency step. This was achieved through the creation of a MATLAB® program that would use the time domain data for the LISN voltages output from the PSPICE® program.

According to the modified version of the CISPR specification used in measurement, the bandwidth of the IF filter to be used is approximately 10kHz, and the frequency steps are 7.5 kHz wide. The frequency range is from 150 kHz to 30 MHz. This yielded approximately 3,980 discrete steps across the entire frequency range.

Although this method yielded the most accurate results at lower frequencies, this method too, was computationally intensive for a simple reason. According to Nyquist's criterion, the sampling frequency of a signal must be at least two times the frequency of interest. In applying the digital filter to the signal, as the frequency of interest increased, so too did the sampling frequency. As frequencies increased, so too did computing times. This was particularly true when a higher order bandpass filter was used. In the duplication of the IF filter characteristics used in the spectrum analyzer, a higher order filter was necessary to duplicate the steep roll-off characteristics of the IF filter.

The final method which was tried, was to pass a sliding window over the time domain data and apply an FFT to the windowed data.

The FFT was performed for each window over the entire frequency range of interest at fixed frequency steps. In this case the conducted RFI was calculated every 7.5 kHz from 150 kHz to 30 MHz. To simulate a peak hold" function of the spectrum analyzer, the FFT values for each window were subsequently compared, and the maximum value of the transform was kept for the particular frequency of interest. The FFT was performed using a rectangular window.

23

In terms of duplicating the characteristics of the IF filter using this method, the FFT was performed using the 10 kHz resolution bandwidth specified. As the filter characteristics of the IF filter in the spectrum analyzer used in experimental measurements possessed a steep roll-off, the shape of the peaks in the simulation were a good approximation for the characteristics of the IF filter used in experimental measurements.

Frequency Domain Results

The FFT results for mid speed operation, and high speed operation for a motor and drive without RFI suppression components appear in Figures 7 and 8 respectively. The straight line passing through the data on both graphs is the specification limit for the frequency range of interest. The darker curves on both graphs are the simulated results.
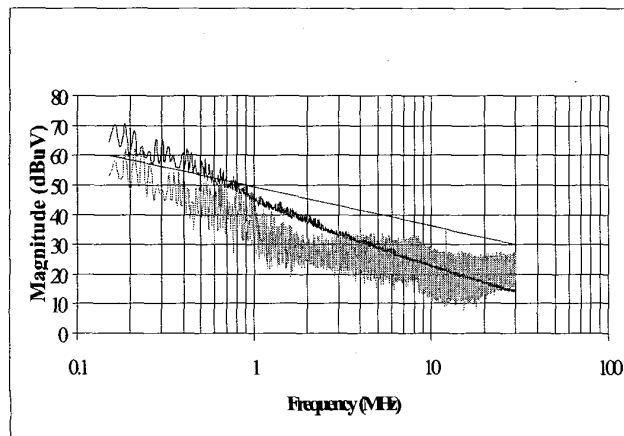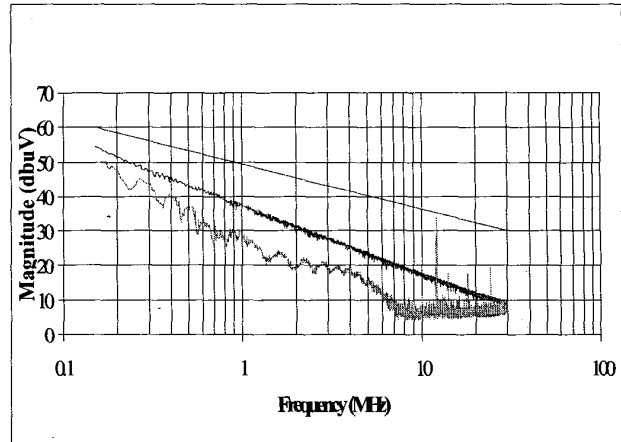
Figure 7. Mid speed conducted RFI spectrum.

As may be seen in the results for mid speed operation, the simulated values follow the same trend as the experimental values, however, at lower frequencies, the simulated values are on average 10dB higher than the experimental values. The difference gradually decreases at higher frequencies, where the situation is reversed. At higher frequencies, the experimental data is greater in magnitude than the simulated data. In addition, the spectrum of the simulated data is more broadband in appearance than that of the experimental data. The discrepancies are attributable to several factors. The frequency domain data results show better the differences between the measurements and simulations of the LISN voltages. Some discrepancy in the frequency domain magnitudes at low frequencies may be due to the inherent differences between the FFT method used in simulation, and experimental measurement. One discrepancy may have to do with the characteristics of the spectrum analyzer peak detector used in measurement.

At high frequencies, the discrepancies may be due to the absence of major PCB trace impedances in the simulation model. Specifically, the PWM waveforms in the motor drive

were generated using a microprocessor with very fast rise and fall times. As a result, this discrepancy may be attributable to conducted noise that was present on the voltage supply for the microprocessor that would not be present in the simulated

model.

Figure 8. High speed conducted RFI spectrum.

In the case of high speed motor operation, the simulated results are on average 10 dB greater in magnitude than the experimental results. Some discrepancies may be attributable to the inherent differences between the simulated and experimental methods of obtaining the frequency spectrum.

Once again, the high speed simulation results appear to be more broadband in nature than the experimental results, decreasing at approximately 20 dB per decade.

During high speed operation, there is no PWM performed on the motor windings. As a result, noise associated with the microcontroller due to PWM will not be present in the high speed results. What is evident, however, in the high speed experimental results is the presence of microcontroller oscillator harmonics in the conducted RFI spectrum. These peaks are narrow band in nature, with the fundamental appearing at 12 MHz, and every 12 MHz thereafter.

Conclusions

From the time domain results, one might conclude that using a lumped parameter measured model is an effective method of predicting the time domain LISN voltages from which a conducted RFI spectrum may be obtained.

As far as frequency domain results are concerned, the correlation between simulated and experimental results show many differences. The simulated results follow the general trend of the experimental results. The discrepancies may be attributable in part, to the methods used to model various motor parameters, and differences between the simulated and experimental methods used to obtain the frequency spectrum.

For example, the phase back EMF's were modeled as the sum of sinusoidal harmonic voltages. In reality, the phase back EMF's are a function of the flux in the air gap. As a result, it

may be more prudent to use a finite element program to determine the flux in air gap under the load conditions of concern so as to incoporate the effects of armature reaction on the shape of the phase back EMF's. Finite element tools could also be used to predict the values in the self and mutual inductance matrix, as well as iron losses.

In addition, in the system of concern, analog, digital, and power electronic components were packaged on a single PCB. In the model, the impedance effects of significant PCB traces were largely ignored.

In comparing the simulated and experimental results, it can be concluded that this method of predicting conducted RFI emissions over the frequency range of interest can serve as a valuable simulation tool that can shorten the development cycle.

At this point in time, simulation has only been conducted on one motor with a winding having a known number of turns, and with a single fan. To further validate the model, another motor winding and fan load should be simulated.

References

[1] Rakotovao, M., Vergine, P., Casaril., D. "Contribution in EMI Case of DC motors: Influence of Brushes-Collector Contact in Conducted Interference", *Society of Automotive Engineers, Convergence '98 Proceedings*, pp 85-92.

[2] Suriano, C.R., Suriano, J.R., Thiele, G., Holmes, T.W., "Prediction of Radiated Emissions From DC Motors", *IEEE Conference Transactions on Electromagnetic Compatibility*, Denver Colorado, August 1998, pp 790 – 795.

[3] Zhong, E., Lipo, T.,A., "Improvements in EMC Performance of Inverter-Fed Motor Drives", *IEEE Transactions on Industry Applications*, Vol. 31, No.6, November/December 1995, pp 1247-1256.

[4] Grandi, G., Casadei, D., Reggianni, U., "Analysis of Common- and Differential-Mode HF Current Components in PWM Inverter-Fed AC Motors" , *PESC98, Record of the 29th Annual Power Electronics Specialist Conference*, Fukuoka, Japan, May 17-22, 1998, pp 1146-1151.

[5] Chen., C, Xu, X., "Modeling the Conducted EMI Emission of an Electric Vehicle (EV) Traction Drive", *IEEE 1998 Proceedings on Electromagnetic Compatibility* , pp 796-801.

[6] Ran., L., Gokani., S., Clare., J., "Conducted Electromagnetic Emissions in Induction Motor Drive Systems Part I: Time Domain Analysis and Identification of Dominant Modes", *IEEE Transactions on Power Electronics*, Vol. 13, No. 4, July 1998. pp 757-767.

[7] Ran., L., Gokani., S., Clare., J., "Conducted Electromagnetic Emissions in Induction Motor Drive Systems Part II: Frequency Domain Models", *IEEE Transactions on Power Electronics*, Vol. 13, No. 4, July 1998. pp 768-775.

[8] Zhu, H., Lai, J-S, Hefner, A.R., Tang, Y, Chen, C., "Analysis of Conducted EMI Emissions from PWM Inverter Based on Empirical Models and Comparative Experiments", *Conference Transactions of IEEE Power Electronics Specialist Conference, PESC 99*, pp 861-867.

[9] Spee, R., Wallace., A.K.," Performance Characteristics of Brushless DC Drives", *IEEE Transactions on Industry Applications*, Vol 24, No. 4, July/August 1988, pp 568-573.

[10] Wallace., A.K., Spee, R., "The Effects of Motor Parameters on the Performance of Brushless DC Drives", *IEEE Transactions on Power Electronics*, Vol 5, No. 1, January 1990, pp 2-8.

[11] Wallace., A.K., Spee, R., "The Simulation of Brushless DC Drive Failures", *IEEE PESC '88 Record*, pp 199-206.

[12] Spee, R., Wallace., A.K., "Performance Characterization of Brushless DC Drives", *IEEE IAS 1987 Proceedings*, pp1-6.

[13] Strahan., R.J., "Energy Conversion by Nonlinear Permanent Magnet Machines", *IEE Proc.-Electr. Power Appl.*, Vol. 145, No. 3, May 1998, pp 103-198.

[14] Zhang, J., Mathew, R., Flinders, F., Oghanna, W., "Simulator of DC Traction Motors Including Both Main and Interpole Saturation", *IEE Proc.-Electr. Power Appl.*, Vol. 145, No. 4, July 1998, pp 377-382.

[15] Jack, A.G., Atkinson, D.J., Slater, H.J., "Real-time Emulation for Power Equipment Development. Part 1: Real Time Simulation", *J., IEE Proc.-Electr. Power Appl.*, Vol. 145, No. 2, March 1998, pp 92-97.

[16] Jack, A.G., Atkinson, D.J., Slater, H.J., "Real-time Emulation for Power Equipment Development. Part 2: Real Time Simulation", *J., IEE Proc.-Electr. Power Appl.*, Vol. 145, No. 2, March 1998, pp 153-158.

[17] Cho, D.-H., Kim, K., "Modeling of Electromagnetic Excitation Forces of Small Induction Motor for Vibration and Noise Analysis", *J., IEE Proc.-Electr. Power Appl.*, Vol. 145, No. 3, May 1998, pp 199-205.

[18] C.D. McGillem, G.R. Cooper, *Continuous and Discrete Signal and System Analysis*, Second Edition, Holt Rinehart and Winston, Toronto, 1984.